Am J Cancer Res 2022;12(12):5484-5499
www.ajcr.us /ISSN:2156-6976/ajcr0145089

Original Article

2,2'-((1R,3R,4S)-4-methyl-4-vinylcyclohexane-1,3-diyl) bis(prop-2-en-1-amine), a bisamino derivative of β-Elemene, inhibits glioblastoma growth through downregulation of YAP signaling

Li-Ying Cao[1,2,3*], Jia-Yun Xu[2,3*], Xiao-Tao Zhuo[2,3], Wei Zhang[2,3], Li-Jia Wei[1,2], Jian-Hong Dong[2,3], Ren-Ren Bai[2,3], Xin Wang[2,3], Yuan-Yuan Jiang[2,3], Yong-Jie Wang[2,3], Xiang-Yang Ye[2,3], Tian Xie[2,3], Zhi-Hui Huang[2,3]

[1]Laboratory of Aging and Cancer Biology of Zhejiang Province, School of Basic Medical Sciences, Hangzhou Normal University, Hangzhou 311121, Zhejiang, China; [2]School of Pharmacy, Hangzhou Normal University, Hangzhou 311121, Zhejiang, China; [3]Key Laboratory of Elemene Class Anti-Cancer Chinese Medicines, Hangzhou Normal University, Hangzhou 311121, Zhejiang, China. [*]Equal contributors.

Received July 2, 2022; Accepted November 20, 2022; Epub December 15, 2022; Published December 30, 2022

Abstract: β-Elemene, a compound extracted from Chinese herb *Curcuma wenyujin*, has been demonstrated with antitumor effects in various cancers, including glioblastoma (GBM), a primary brain tumor with high morbidity and mortality. In this study, we reported a bisamino derivative of β-Elemene, 2, 2'-((1R, 3R, 4S)-4-methyl-4-vinylcyclohexane-1, 3-diyl) bis(prop-2-en-1-amine) (compound 1), displayed a better anti-GBM effect than β-Elemene with lower concentration. GBM cell lines (C6 and U87) were treated with compound 1 and subsequently analyzed by several assays. Compound 1 significantly inhibited the migration of C6 and U87 cells based on wound healing assay, transwell assay and inverted migration assay. Furthermore, colony formation assay, immunostaining and flow cytometry assays revealed that compound 1 significantly inhibited the proliferation of GBM cells. In addition, compound 1 induced the apoptosis of GBM cells. Mechanistically, we found Yes-associated protein (YAP) was down-regulated in compound 1-treated GBM cells, and the overexpression of YAP partially rescued the anti-GBM effects of compound 1. Finally, compound 1 suppresses the GBM growth in xenograft model through inactivation YAP signaling. Taken together, these results reveal that a novel derivative of β-Elemene, compound 1, exhibits more potent anti-GBM activity than β-Elemene through inactivating YAP signaling pathway, which will provide novel strategies for the treatment of GBM.

Keywords: β-Elemene, glioblastoma, YAP, derivative, proliferation, migration

Introduction

Glioblastoma (GBM), astrocytoma grade IV, is the most common and aggressive subset of primary brain tumors, accounting for approximately 52% of all brain neoplasms [1, 2]. GBM is a kind of lethal tumor, characterized by high chemotherapy resistance and diffuse infiltration into the brain tissue and its mean survival is 14 to 15 months [3-5]. Current treatments include surgery, radiotherapy, chemotherapy, molecular targeted therapy, immunotherapy, and traditional Chinese medicine [3]. Despite the numerous advances in the development of cancer therapeutics in recent years, the relative survival estimates for GBM are very poor; less than 5% of patients survive 5 years post diagnosis for the early invasion of GBM into the central nervous system [6, 7]. Besides, the prognosis for patients with GBM remains discouraging as a result of the high therapeutic resistance [8, 9]. Therefore, identifying more promising agents besides the scant existing ones will be critical for improving patients' current situation with GBM.

β-Elemene, a natural product extracted from *Curcuma wenyujin*, has been proved to have a large spectrum of anticancer effects in various types of cancers with limited toxicity [10]. This

essential oil contains a mixture of β-, γ- and δ-elemenes [11]. β-Elemene, as the major active anticancer component in the elemene mixture, demonstrates a potent anti-proliferative effect and induces apoptosis in various types of tumors, including breast, liver and glioma [10, 12-17]. Despite the broad-spectrum curative effect of β-Elemene, its mechanism of action has not been clearly illustrated yet. In general, the main antitumor effects [15] include inhibition of cell proliferation, migration and invasion, induction of apoptosis of cancer cells [18-22]. Dramatically, as a noncytotoxic Class II antitumor drug [23], the biological activity of β-Elemene is moderate or weak [24], and its water solubility and stability is poor [23], indicated by its high IC_{50} value against several tumor cell lines [25, 26]. Several papers have been published devoting the modifications of β-Elemene, seeking better biological activity and improvement of its water solubility [23, 27, 28].

For the same purpose, in this study, we modified the structure of β-Elemene and obtained some derivatives, among which the most effective was compound 1. It has been shown a lower half maximal inhibitory concentration than β-Elemene by CCK8 assay. We then detected the anticancer effect on GBM cells, and found that compound 1 inhibited the migration and invasion, suppressed the proliferation, and induced apoptosis of C6 and U87 cell lines. A subcutaneous xenografted nude mice model showed a better inhibition of tumorigenesis of compound 1 than β-Elemene with a lower dosage.

Material and methods

GBM cell lines

GBM Cell lines C6 and U87, were kindly provided by Prof. Maojin Yao (Sun Yat-Sen University), and were maintained in high glucose Dulbecco's modified eagle medium (Gibco) supplemented with 10% fetal bovine serum (Hyclone), 1% penicillin/streptomycin (Gibco). Cells were cultured under standard culture conditions in an incubator with 5% CO_2 at 37°C.

Plasmids construction and transfection

For YAP, cDNA of YAP was amplified by PCR, (Forward: 5'-CGGAATTCGCCACCATGGATCCCGGGCAGCAG-3', Reverse: 5'-GGCACCGGTACTAACCATGTAAGAAAGC-3'). For YAP shRNA, the target sequence is "GCCACCAAGCTAGATAAAGAA". The plasmids were transfected in C6 cells as the manufacturer's instructions. After transfected for 6 h, the transfection mixture was replaced with fresh growth medium and subsequent experiments with transfected cells were performed after 48 h transfection.

Cell counting kit-8 (CCK8) assay

Cell viability was measured by CCK8 cell counting kit (A311-01/02, Vazyme biotech). In brief, C6 and U87 cells were seeded into 96-well plates of 5000 cells/well and cultured in DMEM of 1% serum with certain concentrations of derivatives of β-Elemene and the control solvent for 24 h, and then, 10 μl CCK8 solution was added to each well and incubated for 2 h. The optical density of the solution was determined by a Microplate Reader (Multiskan MK3, Thermo Scientific) at 450 nm. Five replicate wells were designed for each cell sample.

Immunofluorescent assay

For cultured cells, cells were seeded into 12-well plates with glass slides and cultured with medium containing compound 1 or the control solvent for 24 h. For tumor tissues, the tumors were taken from the nude mice and fixed in 4% paraformaldehyde in 0.01 M phosphate-buffer saline (PBS, pH 7.4) at 4°C for 24 h, then the tumors were immersed in 10%, 15%, 20% sucrose in 0.01 M PBS (pH 7.4) for 1 h respectively and in 30% sucrose overnight at 4°C. Tumors were mounted in Tissue-Tek O.C.T. Compound (SAKURA, O.C.T.4583, USA) and frozen for 1 h, then cut into sections (20 μm) by using a cryostat (CM1900, Leica Biosystems, Germany) and then the sections were mounted on glass slides (servicebio, G6004-1, Wuhan, China) and air-dried for 24 h.

For immunofluorescent labeling, sections were permeabilized with 0.3% Triton X-100 for 30 min and then blocked with 5% bovine serum albumin (BSA) for 30 min at room temperature. Subsequently, sections were then incubated with primary antibody overnight at 4°C. Primary antibodies used included rabbit anti-Ki67 (#AB9260, Merck Millipore, 1:300), rabbit anti-YAP (#14074, CST, 1:500), rabbit anti-cleaved caspase3 (#9661, CST, 1:500). Sections were washed with PBS three times and then

incubated with fluorescently-labeled secondary antibody in the dark at room temperature for 2 h. The sections were washed with PBS and then incubated with DAPI. After being washed three times with PBS, sections were mounted and photographed under a laser scanning confocal microscope (Olympus FV1000, Tokyo, Japan).

Western blot

C6 and U87 cells or tumor tissues obtained from the sacrificed nude mice, were transferred into ice-cold lysis buffer and homogenized with Ultrasonic apparatus (Sonics, USA). Samples were then centrifuged at 4°C, 12,000 g for 10 min, supernatants were concentrated with a BCA (Thermo, Waltham, USA) protein assay. Loading buffer was added to the samples and boiled for 10 min. Proteins were separated on a 10% SDS-page by applying 20 μg total protein for each sample and transferred onto a polyvinylidene fluoride (PVDF) membrane. Membranes were incubated with 5% skimmed milk in PBS to block the non-specific reaction for 1 h at room temperature, after washed with PBS three times, incubated with primary antibody dilution buffer overnight at 4°C. Primary antibodies used included rabbit anti-YAP (#14074, CST, 1:1000), rabbit anti-p-YAP (#4911, CST, 1:1000), rabbit anti-caspase3 (#13008, CST, 1:1000), rabbit anti-cleaved caspase3 (#9661, CST, 1:1000), rabbit anti-cyclinB1 (12231T, CST, 1:1000), rabbit anti-cyclinD1 (55506T, CST, 1:1000), mouse anti-bcl2 (M1206-4, huabio, 1:1000, rabbit anti-bax (ET1603-34, huabio, 1:1000), rabbit anti-Ki67 (#AB9260, Merck Millipore, 1:500); mouse anti-β-actin (200068-8F10, ZENBIO, 1:1000). Membranes were blocked by blocking buffer (5% skimmed milk in PBS) for 30 min at room temperature and then incubated with horseradish peroxidase-conjugated secondary goat anti-rabbit or goat anti-mouse diluted with blocking buffer for 1 h at room temperature, subsequently, the membranes were washed with PBS three times for 10 min each time. Finally, membranes were incubated with supersignal chemiluminescent substrate (Thermo, Waltham, USA) to visualize the binding sites and then exposed using a detector (ChemiDoc MP, Bio-Rad Hercules, America).

Transwell assay

Cells (5×10^4) in serum-free medium were seeded into the upper chamber of a Transwell insert (8-μm pore size; Corning Inc.). The lower chamber was added in a medium with 10% FBS as a chemoattractant. After incubation for 24 h, the serum-free medium in the upper chamber was removed and infiltrated with 4% paraformaldehyde for 15 min, stained with crystal violet for 30 min, washed with PBS, and dried at room temperature. The upper un-migrated cells were gently wiped off with a cotton swab, and counted under microscope.

Colony formation assay

Cells (1000/well) were seeded in a 6-well plate, and cultured for 24 h in culture medium containing 1% FBS and then compound 1 were added, and continuously cultured for 7 d. The culture medium was removed and cells were infiltrated with 4% paraformaldehyde for 15 min, stained with crystal violet, washed with PBS, dried and counted.

Wound healing assay

Cells were seeded in a 6-well plate. After the cells had grown to about 100% confluency, the cell layer was scratched with a sterile yellow Gilson-pipette tip. After scratching, the medium containing 10% FBS was replaced with a serum-free medium. Images of the scratched cells were captured at 0 h and 24 h.

Aggregation migration assay

20 μl cells with high density were plated on coverslip. Immediately, the coverslips inverted with cells hanging downward for 6 h to allow the cells to aggregate, and then the aggregated cells were removed onto larger coverslips coated with matrigel (10 μg/μl, Sigma) and cultured for 2 d to allow cell migration in culture media with or without compound 1. The culture media was removed, cells were fixed, and cell migration distance away from the edge of the fragment was analyzed. The maximum distance of the leading edge of cells was measured in each experiment.

Animals

The experiment performed with animals was approved by the Institutional Animal Care and Use Committee at Hangzhou Normal University. Male nude mice of six-week-old BALB/c were purchased from Shanghai SLAC Laboratory Animal (Co, Ltd), and raised at the Animal

Experimental Center of Hangzhou Normal University.

GBM xenograft model

The cultured C6 cells were inoculated in subcutaneous male BALB/c nude mice, aged about 6 weeks, to establish the *in vivo* GBM at constant temperature (22-25°C). Mice were randomly divided into 2 groups of 5 animals each. When the tumor volume reached approximately 3 mm^3, compound 1 dissolved in PBS, were injected into the subcutaneous of the nude mice every other day. Each group of mice was intravenously injected with the same dose of PBS and compound 1, at the same time, the tumor volume was measured. Animals were fed with heat-sterilized food and water and maintained on sterilized bedding in a homoiothermal specific pathogen-free (SPF) laminar flow cabinet, a vernier caliper was used and the formula $a \times b^2/2$ was performed (a and b represented the length and width of the tumor volume respectively). After 35 d of tumor growth, the nude mice were sacrificed by cervical spondylolysis after anesthesia. The tumors were removed, photographed and immediately weighed. For immunofluorescent analysis, the tumor tissues were soaked in 4% paraformaldehyde and lysed for western blot assay.

Statistical analysis

All experiments were performed at least three independent times. Statistical analyses were performed using image J and GraphPad Prism 8 software. The statistical analysis significance between multiple groups was performed using analysis of variance (ANONA) and the statistical significance between two means was analyzed by student's *t* test. The data were expressed as the means ± standard error of mean (SEM). Differences with $P<0.05$ were considered to be statistically significant.

Results

Compound 1 inhibited the migration of GBM cells with lower IC_{50}

High purity β-Elemene (purity >95%, compound 2) was obtained from elemene extract *via* multicycle preparative HPLC purification. Compound 3 is a biotin-labeled β-elemene derivative. Compound 1 is a bisamino derivative of β-elemene. Both compounds were synthesized from β-elemene in several steps, and the detailed synthesis procedure will be reported else way. Primarily, CCK-8 assay was conducted to evaluate IC_{50} of these derivatives with rat GBM C6 cell line, and found compound 1 presented better efficiency with lower IC_{50} among the three derivatives (**Figure 1A**). According to the IC_{50} values and valid time shown in **Figure 1A**, **1B**, we chose the concentration of 25 μM of compound 1 and 24 h as the efficient time for drug treatment in the following experiments.

β-Elemene has been proved to inhibit the migration of human GBM cell lines [10]. Wound healing experiment was then performed to detect the effect of migration on C6 cells of three derivatives besides β-Elemene. Since the solvent of β-Elemene and compound 1 are different, to exclude the effect of the solvent on cells, the wound healing experiments of compound 1 (25 μM) and β-Elemene (490 μM) were not performed in the same assay and the absolute value of wound healing percentages of them could be different and not comparable due to the cell density and growth status and so on, so we chose the relative data between compound 1 and β-Elemene for comparison. Compared to β-Elemene, compound 1 had better efficiency in inhibiting GBM cell line migration with lower concentrations (**Figure 1C-G**). Taken together, these results suggest that the derivatives of β-Elemene, compound 1 inhibited the migration of C6 cells with lower IC_{50} values.

Compound 1 inhibited the growth and proliferation of GBM cells

To examine the effect of compound 1 on the proliferation of GBM cell lines, Ki67 (a marker for cell proliferation) staining and colony formation assay were performed in C6 and U87 cell lines. As shown in **Figure 2A-C**, the $Ki67^+$ cells significantly decreased in compound 1-treated C6 and U87 cells compared with the control-treated group. Meanwhile, colony formation assay further showed that the numbers of cell clones were also dramatically decreased both in C6 and U87 cells treated with compound 1, compared with control-treated cells. Taken together, these results suggested that compound 1 inhibited the growth and proliferation of GBM cells.

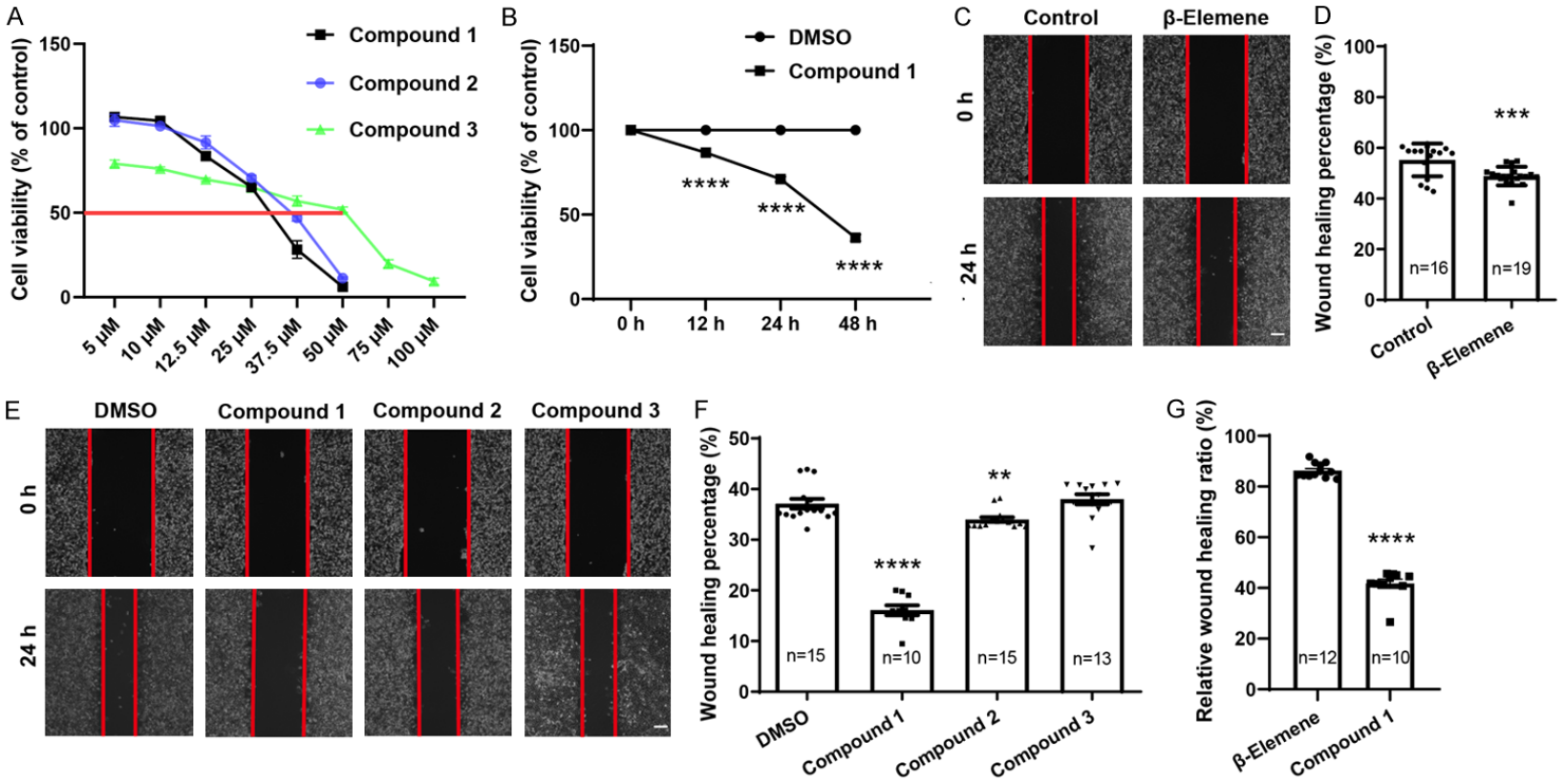

Figure 1. The derivative of β-Elemene, compound 1 inhibited the migration of C6 cells with lower IC_{50}. A. The IC_{50} of the β-Elemene derivatives was measured by CCK-8 (n=5). The rat GBM C6 cells were seeded in 96-well plates at 5×10^3/well and treated with different concentrations (0, 5, 10, 12.5, 25, 37.5, 50, 75, 100 μM) of three derivatives for 24 h for CCK-8 assay. B. CCK-8 assay detected the cell viability of C6 cells treated with compound 1 with a concentration of 25 μM for different time points (12 h, 24 h, 48 h) (n=5). C, E. Wound healing experiment examined the inhibition efficiency of migration in C6 cells between the three derivatives with the concentration of 25 μM and β-Elemene (490 μM). D, F. Quantification of the wound healing percentage of β-Elemene and three derivatives respectively. G. Quantification of the relative inhibition effect of migration of C6 cells treated with compound 1 compared to β-Elemene. Scale bars, 100 μm. Data were mean ± SEM. ***P<0.01, ***P<0.001, ****P<0.0001*.

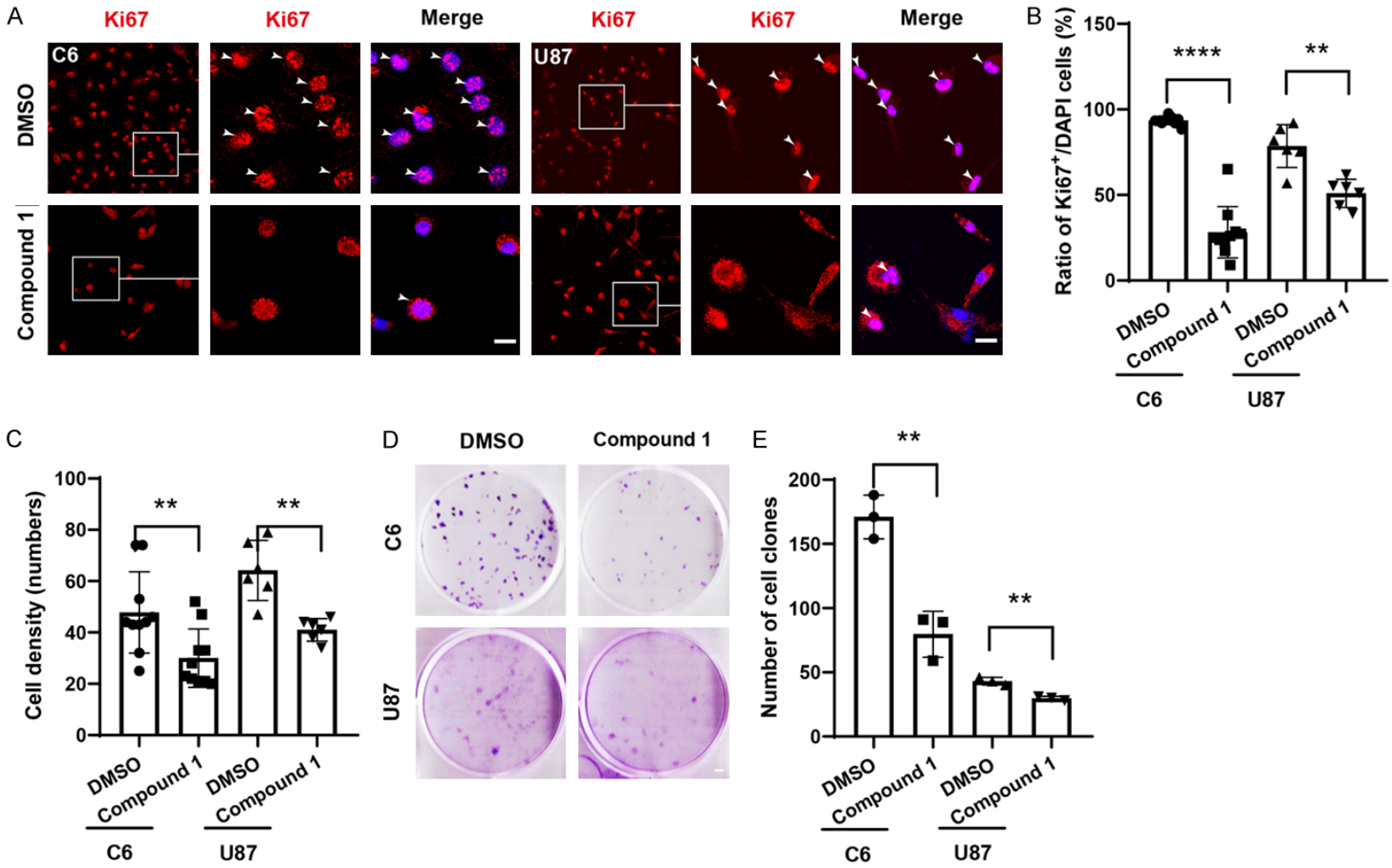

Figure 2. Compound 1 inhibited the growth and proliferation of GBM cells. (A) Immunostaining analysis of Ki67 in C6 and U87cells treated with compound 1. (B, C) Quantification of ratio of Ki67$^+$ (Ki67$^+$/DAPI) cells and cell density respectively as shown in (A) (n=8 and n=6 respectively). (D) Colony formation assay detected the proliferation of C6 and U87 cells treated with compound 1. (E) Quantification of the clone numbers as shown in (D), (n=3). Scale bars, 20 μm in (A) and 2 mm in (D). Data were mean ± SEM. ***P<0.01, ****P<0.001*.

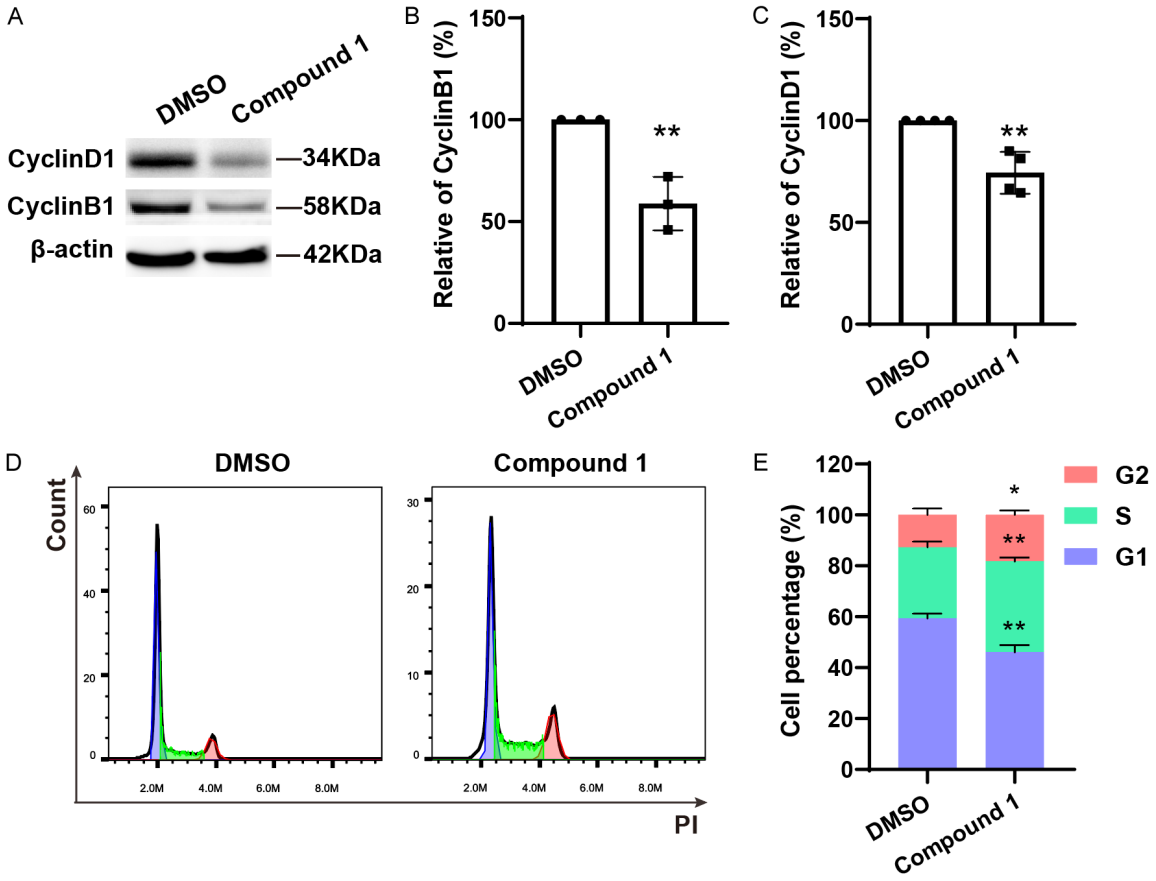

Figure 3. Compound 1 arrested S cell cycle of GBM cells. (A) Represent images of expression of CyclinB1 and CyclinD1 by Western blot in C6 cells treated with compound 1. (B, C) Quantification of protein level of CyclinB1 (B) (n=3) and CyclinD1 (C) (n=4) respectively as shown in (A). (D) Flow cytometry assay with PI staining showed the percentage of each cell cycle phase treated with compound 1. (E) Quantification of percentage of cell cycle phase. Data were mean ± SEM. **P<0.05, **P<0.01*.

Compound 1 arrested S cell cycle in GBM cells

To examine whether compound 1 inhibited cell growth and proliferation by arresting cell cycle, cell-cycle-related proteins were detected by western blot. As shown in **Figure 3A-C**, the expression of cyclinB1 and cyclinD1 were markedly decreased in compound 1 treated C6 cells. Furthermore, the flow cytometry experiment showed that cell cycle progression was arrested at the S phase and retarded from G2/M to G1 after compound 1 treatment (**Figure 3D**, **3E**). Taken toghter, these results suggested that compound 1 inhibited GBM cell growth and cell proliferation by inducing cell cycle arrest at S phase.

Compound 1 induced apoptosis of GBM cells

To examine whether compound 1 can induce the apoptosis of GBM cells, western blot and immunofluorescence assays were performed to detect the expression of apoptosis related proteins. The western blot results showed that protein levels of cleaved-caspase3 (C-caspase3) were significantly increased, whereas, Bcl2/Bax were significantly decreased in compound 1-treated C6 cells (**Figure 4A-C**), indicating that compound 1 treatment increased the expression of pro-apoptosis proteins. Furthermore, immunostaining showed that cleaved-caspase3 positive cells were significantly increased in compound 1-treated C6 cells (**Figure 4D-F**). Flow cytometry experiment with Annexin V/PI staining was then carried out to further test the state of apoptosis induced by compound 1. As shown in **Figure 4G**, **4H**, compound 1 treatment significantly increased the apoptosis of C6 cells. In summary, these results strongly suggested that compound 1 induced the apoptosis of GBM cells.

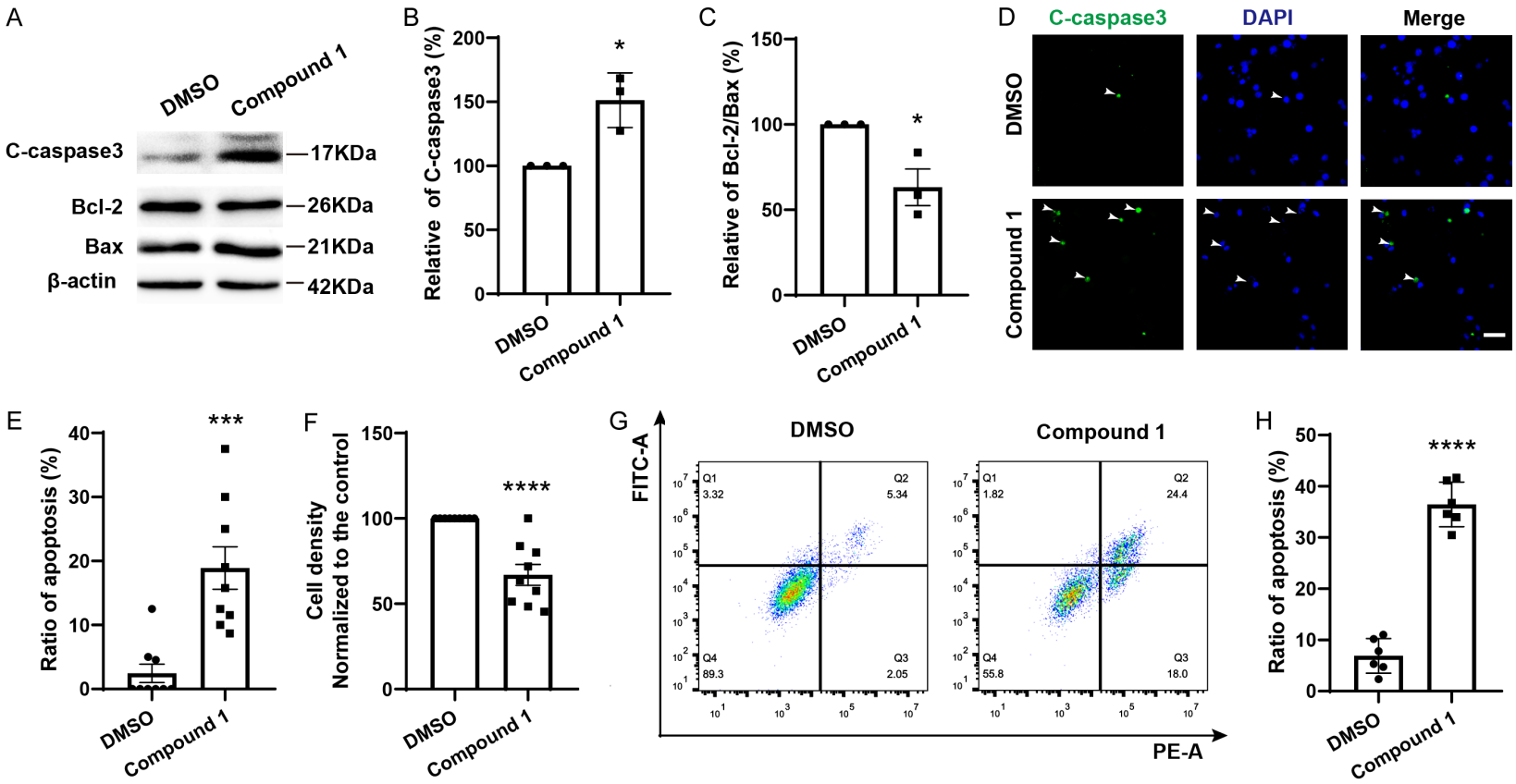

Figure 4. Compound 1 induced apoptosis of GBM cells. (A) Western blot detected the expression of proteins associated with apoptosis in C6 cells treated with compound 1. (B, C) Quantification of the protein level of cleaved-caspase3 (C-caspase3) (B), Bcl2/Bax (C) as shown in (A) (n=3). (D) Immunofluorescent staining of cleaved-caspase3 (C-caspase3) in C6 cells treated with compound 1. (E) Quantification of the percentage of cell apoptosis as shown in (D) (n=9). (F) Quantification of the cell density as shown in (D) (n=9). (G) Flow cytometry assay detected the apoptosis of C6 cells treated with compound 1 and the control. (H) Quantification of the apoptosis ratio as shown in (G) (n=6). Scale bar, 50 μm. Data were mean ± SEM. **P<0.05, ***P<0.001, ****P<0.0001*.

Compound 1 inhibited the migration and invasion of GBM cells

To further examine the inhibitory effect of compound 1 on the migration of GBM cells (**Figure 1E**), C6 and U87 cell lines were performed in this experiment. The results showed that compound 1 treatment significantly inhibited the wound healing in C6 and U87 cells (**Figure 5A**, **5B**). We next carried out transwell assay on these GBM cell lines to further confirm these results. The invasive cells were stained on the lower surface of the plates and counted (**Figure 5C**). Compared with the control-treated group, compound 1 treatment significantly decreased the penetrated cell number (**Figure 5D**). Meanwhile, we also carried out an aggregation migration assay on C6 cells and found the distance and number of migratory cells were markedly decreased in compound 1 treated C6 cells (**Figure 5E-G**), compared with control-treated cells. Taken together, these results strongly suggested that compound 1 inhibited the migration and invasion of GBM cells.

Compound 1 inhibited the proliferation of GBM cells through inactivating YAP signaling

Yes-associated protein (YAP), as a main downstream effector that is negatively regulated by the Hippo pathway, is frequently activated in human malignancies [29], and is required for the growth of glioma [30-32]. Thus we next examined whether YAP signaling was involved in the inhibitive effect of compound 1 on GBM cells. As expected, the expression of YAP was markedly decreased, whereas the protein level of p-YAP/YAP was relatively increased (**Figure 6A-C**). Immunofluorescent assay further showed the relative fluorescence intensity of YAP was significantly decreased in compound 1-treated C6 cells (**Figure 6D**, **6E**). To further examine whether compound 1 treatment inhibited the proliferation of GBM cells through inactivating YAP signaling, a plasmid of YAP with GFP-tag was constructed (**Figure 6F**), and the cell-cycle related protein cyclinB1 and cyclinD1 were significantly elevated in these GFP-YAP transfected C6 cells (**Figure 6F-H**). Meanwhile, overexpression of GFP-YAP partially restored the anti-proliferation effects of compound 1 on C6 cells (**Figure 6I**, **6J**). Besides, the proliferation of C6 cells were inhibited when transfected with plasmid of shRNA-YAP tagged with GFP, and compound 1 exhibited no effect on the proliferation of cells that knocked down of YAP compared with the control group (**Figure 6K**, **6L**). The knock down efficiency of YAP was presented in Supplementary Figure 1. These results suggested that compound 1 inhibited the proliferation of GBM cells through inactivating YAP signaling.

To elucidate the simulated mechanism of compound 1 binding, we tried to use the structure-based drug design tool to dock it inside the YAP protein with protein data bank code (3KYS) to validate the YAP signaling pathway. Full analysis of drug-target interactions of compound 1, with binding energies, three dimensional interactions are summarized in Supplementary Figure 2. Compound 1 was docked within the YAP protein and the binding energy was -7.38 Kcal/mol, and it formed one hydrogen bonds (HB) interactions with PHE-95 as the key interacting amino acid (Supplementary Table 1).

Compound 1 inhibited the tumorigenesis of GBM cells in vivo

Given the *in vitro* data demonstrated the effect of compound 1 on GBM cells, to further investigate the effect of compound 1 on GBM *in vivo*, a tumor xenograft was constructed by injecting C6 cells into nude mice. When C6 cells were grown to approximately 3 mm^3 about 7 d after injection, compound 1 with a 25 mg/kg concentration was injected intraperitoneally into the tumor-bearing mice, meanwhile, the same concentration of β-Elemene group was carried out for comparison. The tumor size was measured every other day for 35 d from the day on drug administration. Afterwards, mice were sacrificed and the tumor tissues were taken out from the mice as shown in **Figure 7A**, **7B**. The weight of tumor tissue was significantly declined (**Figure 7C**). Similarly, the tumor volume was also reduced from 19 d after compound 1 administration (**Figure 7D**), compared with control treated mice, which indicating compound 1 inhibited GBM tumorigenesis *in vivo*. We also monitored the body weight of mice while drug administration, and found that compound 1 did not affect the body weight compared with the control group (**Figure 7E**). However, β-Elemene with the concentration of 25 mg/kg showed no

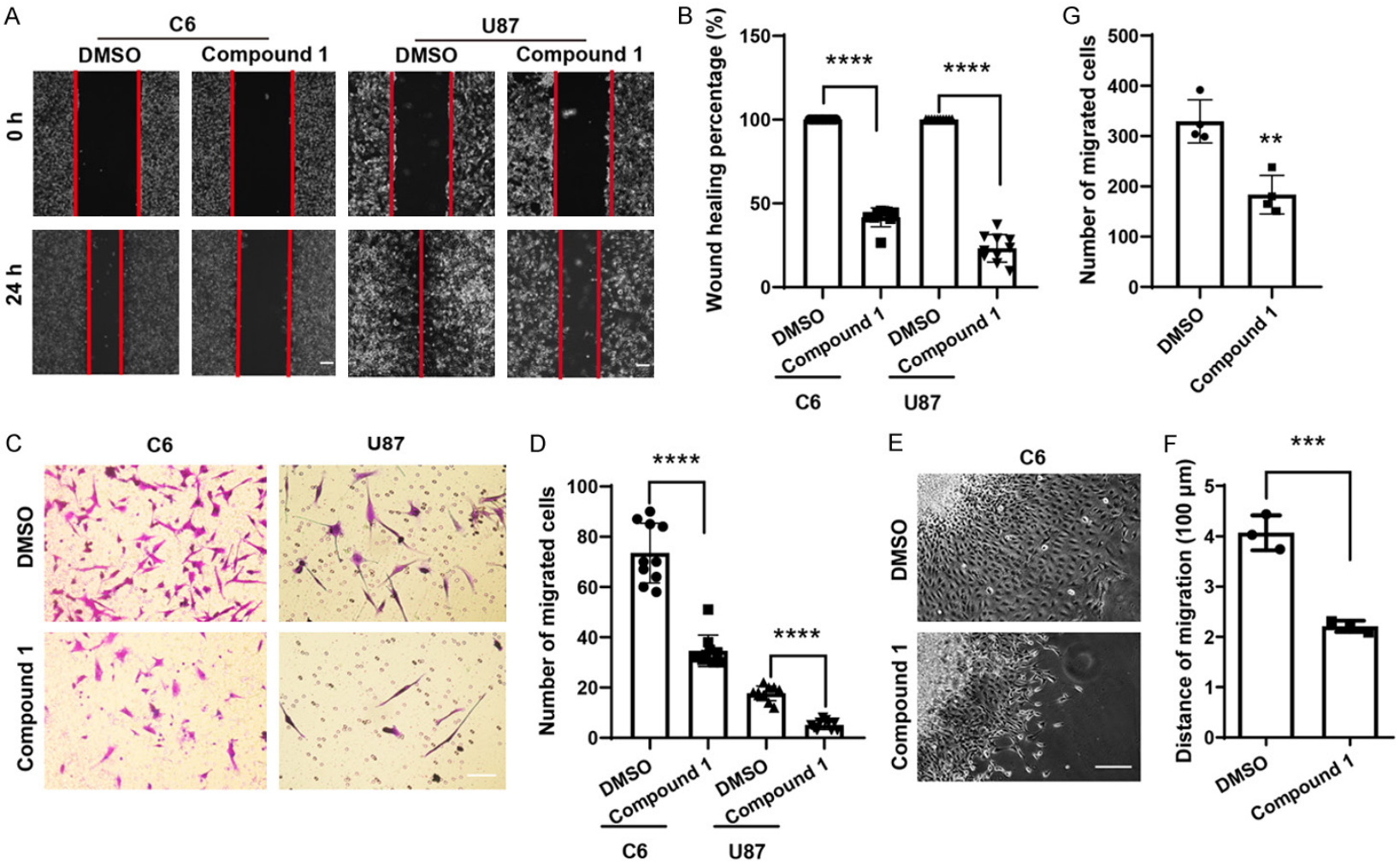

Figure 5. Compound 1 inhibited the migration and invasion of C6, U87 GBM cells. (A) Wound healing experiment performed on C6 and U87 GBM cells treated with compound 1. (B) Quantification of wound healing percentage as shown in (A), (n=10). (C) Typical images of C6 and U87 GBM cells in transwell migration assay. Cells treated with compound 1 for 24 h and then stained with crystal violet and images were captured. (D) Quantification of the number of migrated cells as shown in (C), (n=10). (E) Aggregation migration assay detected the migration of C6 cells treated with compound 1. (F, G) Quantification of the distance and numbers of the migrated cells as shown in (E), (n=3). Scale bars, 100 μm. Data were mean ± SEM. ***P<0.01, ***P<0.001, ****P<0.0001*.

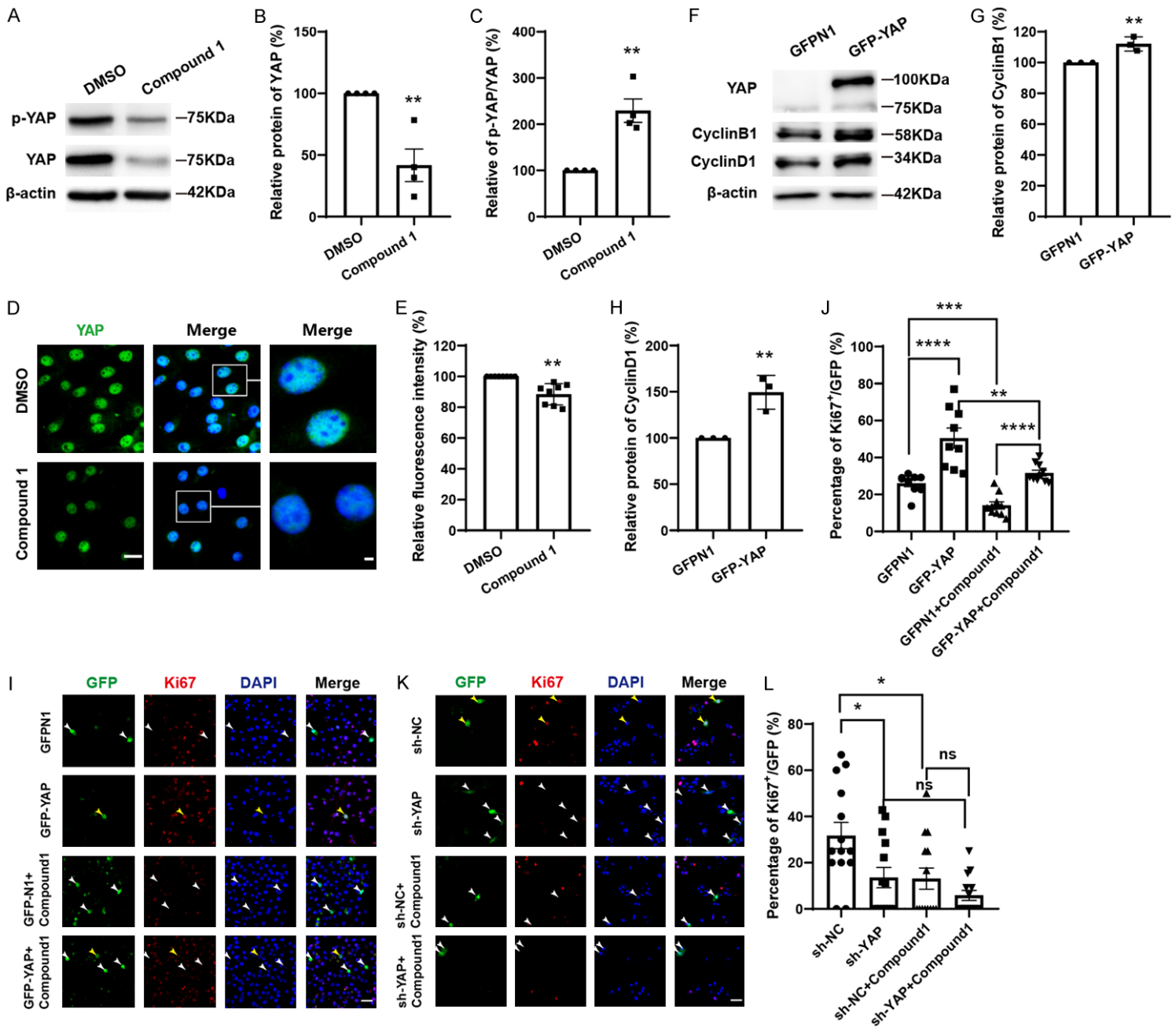
A
DMSO
Compound 1
p-YAP
YAP
β-actin
—75KDa
—75KDa
—42KDa
B
Relative protein of YAP (%)
150
100
50
0
**
DMSO
Compound 1
C
Relative of p-YAP/YAP (%)
400
300
200
100
0
**
DMSO
Compound 1
F
GFPN1
GFP-YAP
YAP
CyclinB1
CyclinD1
β-actin
—100KDa
—75KDa
—58KDa
—34KDa
—42KDa
G
Relative protein of CyclinB1 (%)
120
100
80
60
40
20
0
**
GFPN1
GFP-YAP
D
YAP
Merge
Merge
DMSO
Compound 1
E
Relative fluorescence intensity (%)
120
100
80
60
40
20
0
**
DMSO
Compound 1
H
Relative protein of CyclinD1 (%)
200
150
100
50
0
**
GFPN1
GFP-YAP
J
Percentage of Ki67+/GFP (%)
100
80
60
40
20
0
***
****
**
****
GFPN1
GFP-YAP
GFPN1+Compound1
GFP-YAP+Compound1
I
GFP
Ki67
DAPI
Merge
GFPN1
GFP-YAP
GFP-N1+ Compound1
GFP-YAP+ Compound1
K
GFP
Ki67
DAPI
Merge
sh-NC
sh-YAP
sh-NC+ Compound1
sh-YAP+ Compound1
L
Percentage of Ki67+/GFP (%)
80
60
40
20
0
*
*
ns
ns
sh-NC
sh-YAP
sh-NC+Compound1
sh-YAP+Compound1

Figure 6. Compound 1 inhibited the proliferation of GBM cells through inactivating YAP signaling. (A) Western blot detected the protein level of YAP and p-YAP in C6 cells treated with or without compound 1. (B, C) Quantification of the relative level of YAP and p-YAP/YAP as shown in (A) (n=4). (D) Immunofluorescent staining of YAP in C6 cells treated with compound 1 and the control. (E) Quantification of the fluorescence intensity of YAP as shown in (D) (n=8). (F) Western blot detected the protein level of cyclinB1 and cyclinD1 in C6 cells transfected with GFP-YAP or GPFN1 for 48 h. (G, H) Quantification of the protein level of cyclinB1 and cyclinD1 respectively as shown in (F) (n=3). (I, J) Immunofluorescent staining of Ki67 in C6 cells transfected with GFP or GFP-YAP or shRNA-control (sh-NC) or shRNA-YAP (sh-YAP) with or without compound 1 treatment. (K, L) Quantification of percentage of $Ki67^{+}$/GFP cells. White arrows indicated cells transfected with GFP labeled plasmids that not co-localized with Ki67 and yellow arrows indicated with GFP labeled plasmids that co-localized with Ki67. Scale bar, 20 μm, enlarged scale bar, 5 μm in (D) and 50 μm in (I, K). Data were mean ± SEM. **P<0.05, **P<0.01, ***P<0.001, ****P<0.0001.*

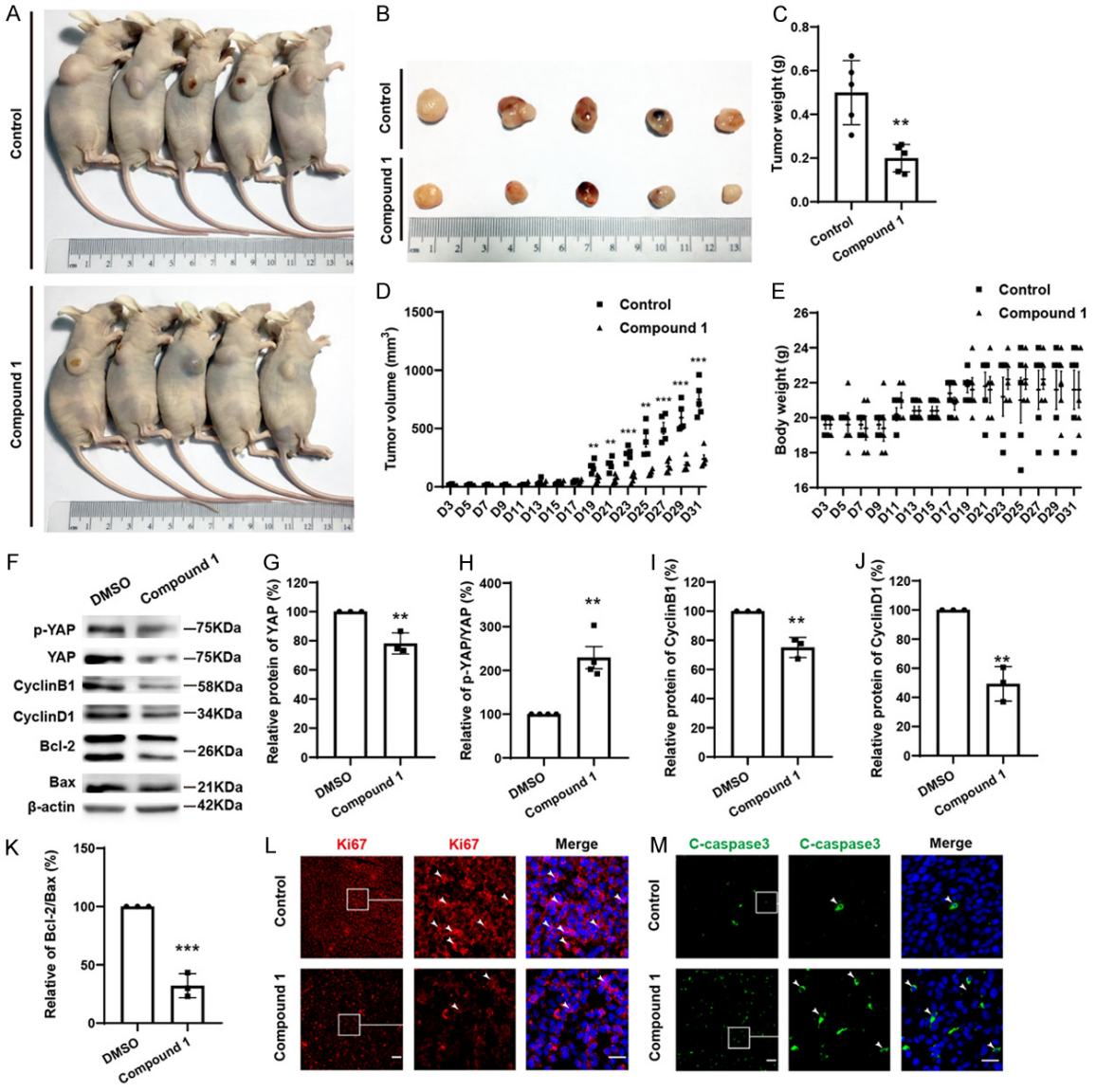

Figure 7. Compound 1 inhibited GBM tumorigenesis in xenografted nude mice. (A) The image of the sacrificed mice treated with the control or compound 1. (B) Image of the tumor issues that were taken from the sacrificed mice treated with the control or compound 1. (C, D) Quantification of the tumor weight and volume between compound 1 treated and the control group (n=5). (E) Quantification of the body weight of the tumor bearing mice that monitored every other day (n=5). (F) Western blot detected the expression of proteins YAP, p-YAP, YAP, cyclinB1, cyclinD1, Bcl2 and bax in the tumor tissues treated with the control or compound 1. (G-K) Quantification of relative protein level of YAP (G) (n=3), p-YAP/YAP (H) (n=4), cyclinB1 (I) (n=3), cyclinD1 (J) (n=3), Bcl2/bax (K), as shown in (F). (L, M) Immunofluorescent staining of Ki67 and cleaved-caspase3 in the tumor tissues treated with compound 1 or the control. Scale bar, 50 μm and enlarged scale bar, 20 μm. Data were mean ± SEM. ***P<0.01, ***P<0.001*.

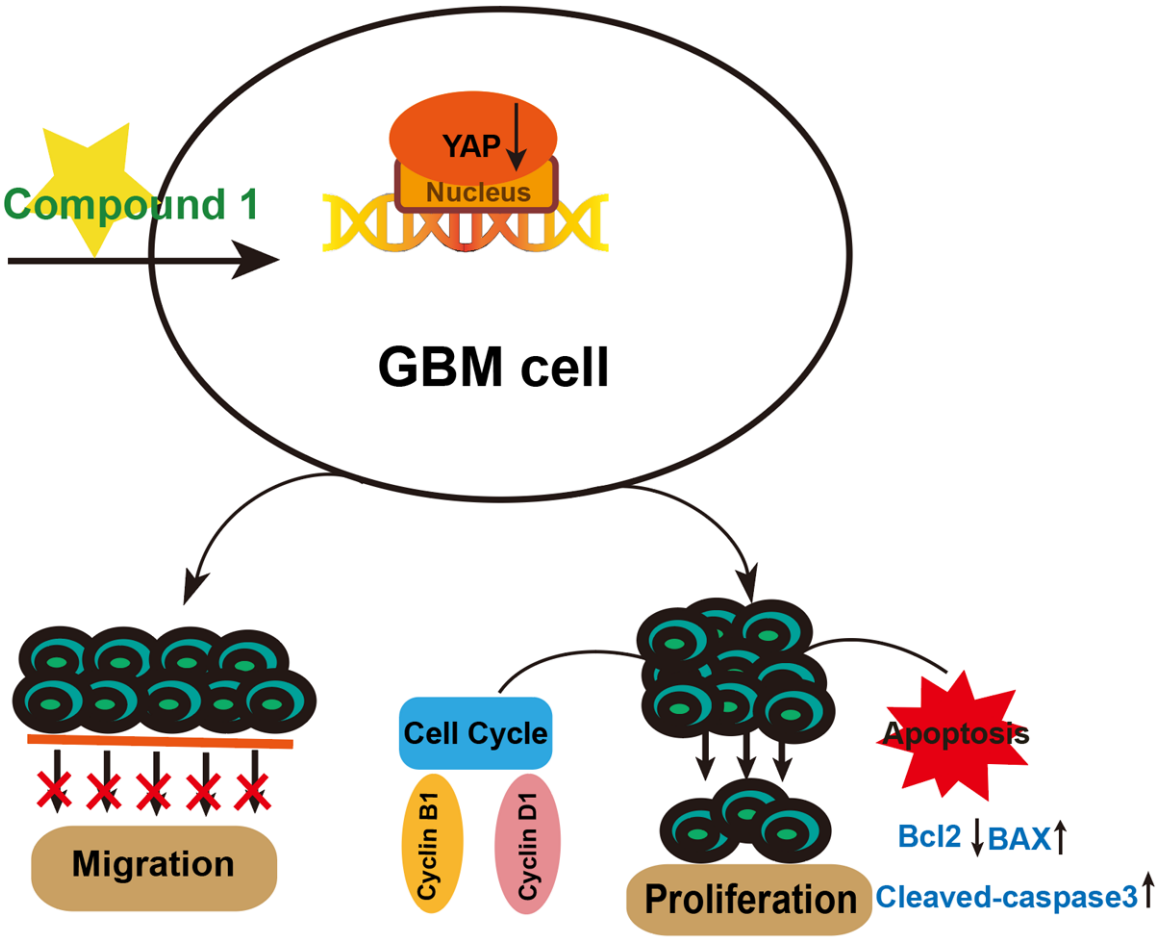

Figure 8. Working model of the functions of compound 1 in GBM through inactivating YAP signaling. Compound 1 inhibits the migration and induces the apoptosis of GBM cells. YAP is inactivated when treated with compound 1, thus, inhibits the proliferation of GBM cells. Furthermore, when YAP is overexpressed, the inhibition effect of proliferation of GBM cells can be partially rescued.

significance in effect on the tumorigenesis compared with the control group, data were shown in Supplementary Figure 3. Consistent with the results of *in vitro* experiments, western blot demonstrated that the YAP, cyclin B1, cyclin D1 and Bcl-2/Bax levels were significantly decreased in compound 1-treated mice, compared with control treatment (**Figure 7F-K**). Furthermore, we continued to evaluate the proliferation and apoptosis of the tumor tissue cells. Again, compound 1 treatment reduced the proliferative cells and induced apoptosis of the GBM tumor tissue (**Figure 7L**, **7M**). In conclusion, these results suggested that compound 1 inhibited the tumorigenesis of GBM *in vivo*.

Discussion

Here, we reported that a bisamino derivative of β-Elemene compound 1 showed better efficiency in inhibiting tumorigenesis of GBM with more effective biological activity than β-Elemene. We also revealed the inhibition of GBM for compound 1 through inactivating YAP signaling in a working model (**Figure 8**).

Previous studies have reported that β-Elemene, displayed a wide spectrum of antitumor effect, clinically used as a second line antitumor drug, which usually combined with fist-line drugs for synergistic effects for years [33, 34]. β-Elemene is good for curative of cancer with multifold effects with low toxicity. However, its biological activity is moderate or weak, indicating high IC_{50} value when working in several tumor cell lines. In this research, we synthesized some derivatives of β-Elemene based on its structure and found compound 1, demonstrated lower IC_{50} than β-Elemene and other derivatives, which performed better efficiency on inhib-

iting the migration of GBM cells. Herein, A series assays were carried out to detect further the antitumor effect of compound 1 on GBM cell lines. We observed the antitumor effect of compound 1 on GBM cells both *in vitro* and *in vivo*. The results manifested that compound 1 inhibited the growth and proliferation, migration and invasion, induced apoptosis, promoted cell cycle arrest in GBM cells and suppressed GBM tumorigenesis in xenografted nude mice.

Although there were different cellular pathways about the effect that β-Elemene acted on different cancers, the mechanism has not been clearly demonstrated yet. In this research, we reported the Hippo signaling pathway, a conserved pathway that could lead to cancer when dysregulated. As a translational coactivator, YAP is negatively regulated by Hippo pathway and controls the size of multiple organs through regulating cell differentiation, proliferation and apoptosis. Excessive YAP activation will cause cell proliferation, thus giving rise to brain tumors that are often lethal, such as neuroblastoma and medulloblastoma [35-37]. Several papers also reported YAP promoted tumor progression of GBM through regulating or regulated by different molecules [30, 38-40]. Recently, Konstantin Masliantsev et al reviewed the Hippo pathway involvement in tumor progression and resistance to treatment of GBM and drugs mainly approaches this pathway targeted indirectly to YAP have been designed [32]. In this study, we examined the expression of YAP after administrating compound 1 and found it was significantly reduced. When YAP was overexpressed, it partially rescued the anti-GBM effects of compound 1, indicating inactivation of YAP signaling pathway participated in the antitumor effect of compound 1. However, the specific molecules that are regulated in Hippo/YAP pathway need further investigation.

In summary, we synthesized the derivative of β-Elemene, compound 1, with a much lower efficient concentration (25 μM) than the effective general concentration of β-Elemene that has been reported both in vitro and *in vivo* [41, 42]. In addition, we also obtained a water-soluble form of compound 1 for *in vivo* experiment to achieve better biology activity with lower toxicity. However, further research on patients still needs to test whether compound 1 could be put into clinical use.

Acknowledgements

This work was supported by the grant from the National Natural Science Foundation of China (92049104, 81801102, 81730108, and 81973635), Scientific Research Foundation for Scholars of Hangzhou Normal University (4125C5021920435, 4125C5021920453 and 2019QDL003), Hangzhou City "115" plan to introduce overseas intelligence projects (20200215 and 20210120), the General Scientific Research Project of Zhejiang Provincial Department of Education in 2021 (Y202147589), and the Ministry of Science and Technology of China (High-end foreign experts program, G20200217005 and G2021017004).

Disclosure of conflict of interest

None.

Address correspondence to: Xiang-Yang Ye, Tian Xie and Zhi-Hui Huang, School of Pharmacy, Hangzhou Normal University, Hangzhou 311121, Zhejiang, China. E-mail: xyye@hznu.edu.cn (XYY); xbs@hznu.edu.cn (TX); huang0069@hznu.edu.cn (ZHH)

References

[1] Yang K, Niu L, Bai Y and Le W. Glioblastoma: targeting the autophagy in tumorigenesis. Brain Res Bull 2019; 153: 334-340.
[2] Kanderi T and Gupta V. Glioblastoma Multiforme. In: editors. StatPearls. Treasure Island (FL): StatPearls Publishing.
[3] Zhang H, Wang R, Yu Y, Liu J, Luo T and Fan F. Glioblastoma treatment modalities besides surgery. J Cancer 2019; 10: 4793-4806.
[4] Silantyev AS, Falzone L, Libra M, Gurina OI, Kardashova KS, Nikolouzakis TK, Nosyrev AE, Sutton CW, Mitsias PD and Tsatsakis A. Current and future trends on diagnosis and prognosis of glioblastoma: from molecular biology to proteomics. Cells 2019; 8: 863.
[5] Mooney J, Bernstock JD, Ilyas A, Ibrahim A, Yamashita D, Markert JM and Nakano I. Current approaches and challenges in the molecular therapeutic targeting of glioblastoma. World Neurosurg 2019; 129: 90-100.
[6] Liu S, Zhou L, Zhao Y and Yuan Y. Beta-elemene enhances both radiosensitivity and chemosensitivity of glioblastoma cells through the inhibition of the ATM signaling pathway. Oncol Rep 2015; 34: 943-951.
[7] Batash R, Asna N, Schaffer P, Francis N and Schaffer M. Glioblastoma multiforme, diagnosis and treatment; recent literature review. Curr Med Chem 2017; 24: 3002-3009.

[8] Chaul-Barbosa C and Marques DF. How we treat recurrent glioblastoma today and current evidence. Curr Oncol Rep 2019; 21: 94.
[9] Strepkos D, Markouli M, Klonou A, Piperi C and Papavassiliou AG. Insights in the immunobiology of glioblastoma. J Mol Med (Berl) 2020; 98: 1-10.
[10] Alizada M, Li J, Aslami H, Yang D, Korchuganova T and Xu YH. β-elemene inhibits the proliferation and migration of human glioblastoma cell lines via suppressing ring finger protein 135. Balkan J Med Genet 2020; 23: 43-49.
[11] Zhu T, Zhao Y, Zhang J, Li L, Zou L, Yao Y and Xu Y. Ss-elemene inhibits proliferation of human glioblastoma cells and causes cell-cycle G0/G1 arrest via mutually compensatory activation of MKK3 and MKK6. Int J Oncol 2011; 38: 419-426.
[12] Zhu TZ, Li XM, Luo LH, Xu YH, Cao P, Liu Y and Liang GB. Beta-elemene inhibits proliferation through crosstalk between glia maturation factor beta and extracellular signalregulated kinase 1/2 and impairs drug resistance to temozolomide in glioblastoma cells. Mol Med Rep 2014; 10: 1122-1128.
[13] Su P and Ahmad B. β-elemene enhances the chemotherapeutic effect of 5-fluorouracil in triple-negative breast cancer via PI3K/AKT, RAF-MEK-ErK, and NF-κB signaling pathways. Onco Targets Ther 2020; 13: 5207-5222.
[14] Gong M, Liu Y, Zhang J, Gao YJ, Zhai PP, Su X, Li X, Li Y, Hou L and Cui XN. β-elemene inhibits cell proliferation by regulating the expression and activity of topoisomerases I and IIα in human hepatocarcinoma HepG-2 cells. Biomed Res Int 2015; 2015: 153987.
[15] Guan C, Liu W, Yue Y, Jin H, Wang X and Wang XJ. Inhibitory effect of β-elemene on human breast cancer cells. Int J Clin Exp Pathol 2014; 7: 3948-3956.
[16] Zhang X, Zhang Y and Li Y. β-elemene decreases cell invasion by upregulating E-cadherin expression in MCF-7 human breast cancer cells. Oncol Rep 2013; 30: 745-750.
[17] Li X, Lin Z, Zhang B, Guo L, Liu S, Li H, Zhang J and Ye Q. β-elemene sensitizes hepatocellular carcinoma cells to oxaliplatin by preventing oxaliplatin-induced degradation of copper transporter 1. Sci Rep 2016; 6: 21010.
[18] Zhao L, Wei J, Wang S, Lang T, Shi X, Shan Z and Teng W. Beta-elemene inhibits differentiated thyroid carcinoma metastasis by reducing cellular proliferation, metabolism and invasion ability. Ann Transl Med 2020; 8: 1232.
[19] Gan D, He W, Yin H and Gou X. β-elemene enhances cisplatin-induced apoptosis in bladder cancer cells through the ROS-AMPK signaling pathway. Oncol Lett 2020; 19: 291-300.
[20] Wang L, Zhao Y, Wu Q, Guan Y and Wu X. Therapeutic effects of β-elemene via attenuation of the Wnt/β-catenin signaling pathway in cervical cancer cells. Mol Med Rep 2018; 17: 4299-4306.
[21] Wang Z, Wang Z, Du C, Zhang Y, Tao B and Xian H. β-elemene affects angiogenesis of infantile hemangioma by regulating angiotensin-converting enzyme 2 and hypoxia-inducible factor-1 alpha. J Nat Med 2021; 75: 655-663.
[22] Xie Q and Li F. The antitumor efficacy of β-elemene by changing tumor inflammatory environment and tumor microenvironment. Biomed Res Int 2020; 2020: 6892961.
[23] Zhai B, Zeng Y, Zeng Z, Zhang N, Li C, Zeng Y, You Y, Wang S, Chen X, Sui X and Xie T. Drug delivery systems for elemene, its main active ingredient β-elemene, and its derivatives in cancer therapy. Int J Nanomedicine 2018; 13: 6279-6296.
[24] He X and Zhuo XT. β-Elemene derivatives produced from SeO(2)-mediated oxidation reaction. R Soc Open Sci 2020; 7: 200038.
[25] Li QQ, Wang G, Zhang M, Cuff CF, Huang L and Reed E. Beta-elemene, a novel plant-derived antineoplastic agent, increases cisplatin chemosensitivity of lung tumor cells by triggering apoptosis. Oncol Rep 2009; 22: 161-170.
[26] Zhu T, Zhao Y, Zhang J, Li L, Zou L, Yao Y and Xu Y. β-elemene inhibits proliferation of human glioblastoma cells and causes cell-cycle G0/G1 arrest via mutually compensatory activation of MKK3 and MKK6. Int J Oncol 2011; 38: 419-426.
[27] Chen J, Wang T, Xu S, Lin A, Yao H, Xie W, Zhu Z and Xu J. Novel hybrids of natural β-elemene bearing isopropanolamine moieties: synthesis, enhanced anticancer profile, and improved aqueous solubility. Fitoterapia 2017; 120: 117-125.
[28] Chen J, Wang R, Wang T, Ding Q, Khalil A, Xu S, Lin A, Yao H, Xie W, Zhu Z and Xu J. Antioxidant properties of novel dimers derived from natural β-elemene through inhibiting H(2)O(2)-induced apoptosis. ACS Med Chem Lett 2017; 8: 443-448.
[29] Liu H, Du S, Lei T, Wang H, He X, Tong R and Wang Y. Multifaceted regulation and functions of YAP/TAZ in tumors (Review). Oncol Rep 2018; 40: 16-28.
[30] Yu OM, Benitez JA, Plouffe SW, Ryback D, Klein A, Smith J, Greenbaum J, Delatte B, Rao A, Guan KL, Furnari FB, Chaim OM, Miyamoto S and Brown JH. YAP and MRTF-A, transcriptional co-activators of RhoA-mediated gene expression, are critical for glioblastoma tumorigenicity. Oncogene 2018; 37: 5492-5507.
[31] Liu Z, Yee PP, Wei Y, Liu Z, Kawasawa YI and Li W. Differential YAP expression in glioma cells

induces cell competition and promotes tumorigenesis. J Cell Sci 2019; 132: jcs225714.
[32] Masliantsev K, Karayan-Tapon L and Guichet PO. Hippo signaling pathway in gliomas. Cells 2021; 10: 184.
[33] Feng HB, Wang J, Jiang HR, Mei X, Zhao YY, Chen FR, Qu Y, Sai K, Guo CC, Yang QY, Zhang ZP and Chen ZP. β-elemene selectively inhibits the proliferation of glioma stem-like cells through the downregulation of notch1. Stem Cells Transl Med 2017; 6: 830-839.
[34] Hu T and Gao Y. β-elemene against Burkitt's lymphoma via activation of PUMA mediated apoptotic pathway. Biomed Pharmacother 2018; 106: 1557-1562.
[35] Shim J and Lee JY. YAP-mediated repression of hrk regulates tumor growth, therapy response, and survival under tumor environmental stress in neuroblastoma. Cancer Res 2020; 80: 4741-4753.
[36] Geng C, Wei J and Wu C. Yap-Hippo pathway regulates cerebral hypoxia-reoxygenation injury in neuroblastoma N2a cells via inhibiting ROCK1/F-actin/mitochondrial fission pathways. Acta Neurol Belg 2020; 120: 879-892.
[37] Fernandez LA, Squatrito M, Northcott P, Awan A, Holland EC, Taylor MD, Nahlé Z and Kenney AM. Oncogenic YAP promotes radioresistance and genomic instability in medulloblastoma through IGF2-mediated Akt activation. Oncogene 2012; 31: 1923-1937.
[38] Zhao M, Zhang Y, Jiang Y, Wang K, Wang X, Zhou D, Wang Y, Yu R and Zhou X. YAP promotes autophagy and progression of gliomas via upregulating HMGB1. J Exp Clin Cancer Res 2021; 40: 99.
[39] Holmes B, Benavides-Serrato A, Saunders JT, Kumar S, Nishimura RN and Gera J. mTORC2-mediated direct phosphorylation regulates YAP activity promoting glioblastoma growth and invasive characteristics. J Neurooncol 2021; 23: 951-965.
[40] Lee H, Hwang SJ, Kim HR, Shin CH, Choi KH, Joung JG and Kim HH. Neurofibromatosis 2 (NF2) controls the invasiveness of glioblastoma through YAP-dependent expression of CYR61/CCN1 and miR-296-3p. J Exp Clin Cancer Res 2016; 1859: 599-611.
[41] Yang D, Xu X, Wang X, Feng W, Shen X, Zhang J, Liu H, Xie C, Wu Q, Miao X, Guo Y, Cai H, Wu L, Zhou S, Yao X, Wang Y, Xie T and Huang Z. β-elemene promotes the senescence of glioma cells through regulating YAP-CDK6 signaling. Am J Cancer Res 2021; 11: 370-388.
[42] Li CL, Chang L, Guo L, Zhao D, Liu HB, Wang QS, Zhang P, Du WZ, Liu X, Zhang HT, Liu Y, Zhang Y, Xie JH, Ming JG, Cui YQ, Sun Y, Zhang ZR and Jiang CL. Beta-elemene induces caspase-dependent apoptosis in human glioma cells in vitro through the upregulation of Bax and Fas/FasL and downregulation of Bcl-2. Asian Pac J Cancer Prev 2014; 15: 10407-10412.

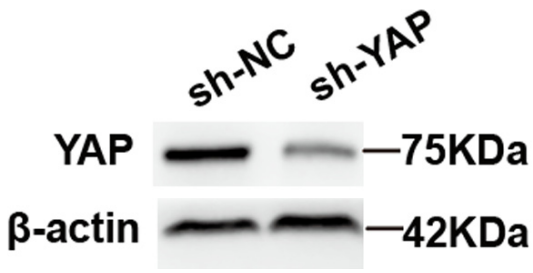

Supplementary Figure 1. Western blot showed the efficiency of knocking down of YAP in C6 cells. Cells were transfected with the plasmids of shRNA-YAP (sh-YAP) and the control shRNA (sh-NC) for 48 h and then lysed for western blot assay.

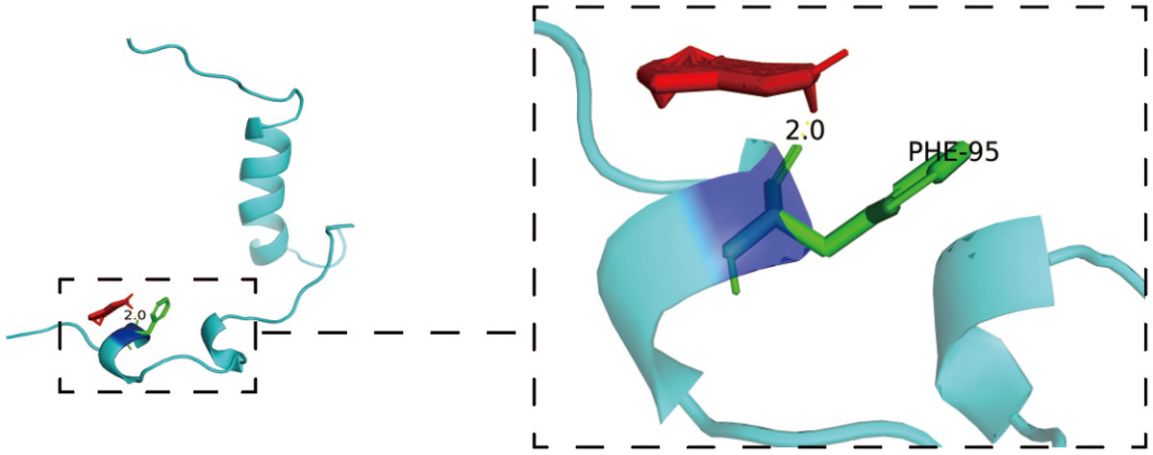

Supplementary Figure 2. Three-dimensional disposition of compound 1 with interactive amino acid.

Supplementary Table 1. Summary of molecular docking stimulations of compound 1

Docked compound	Docking Energy (Kcal/mol)	Drug-Target Interactions
compound 1	-7.38	1 HB with PHE-95

HB: Hydrogen Bone; mol: mole.

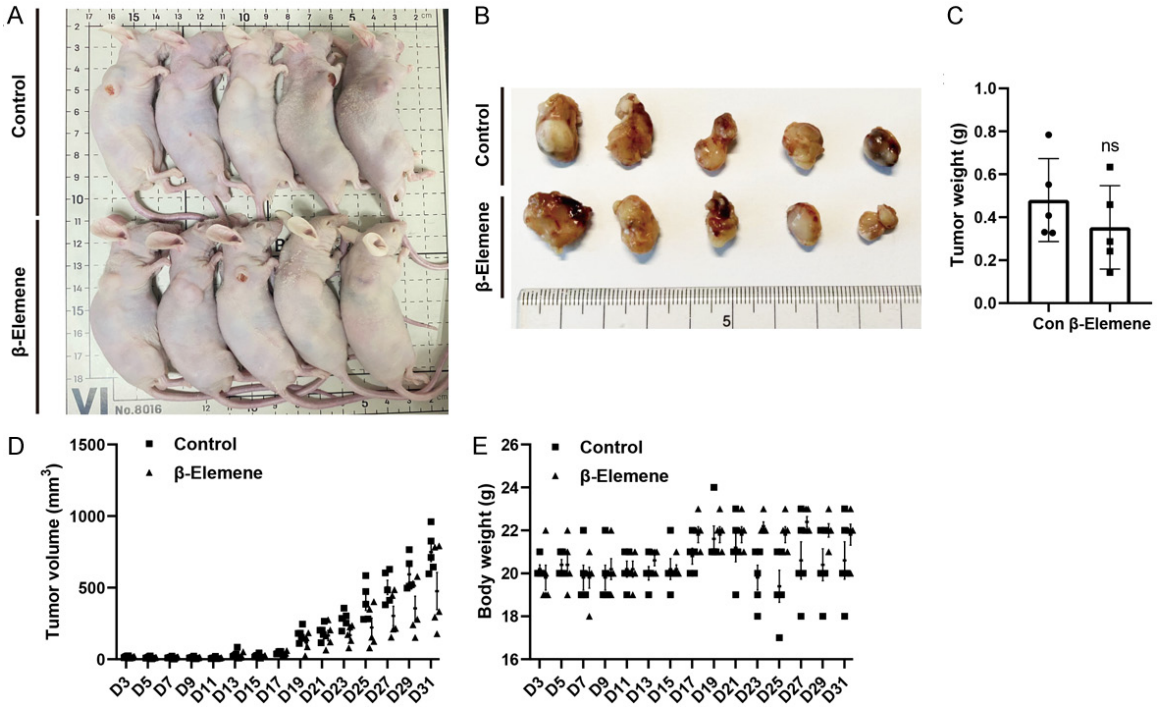

Supplementary Figure 3. A. The image of the sacrificed mice treated with the control or β-Elemene. B. Image of the tumor issues that were taken from the sacrificed mice treated with the control or β-Elemene. C, D. Quantification of the tumor weight and volume between β-Elemene treated and the control group (n=5). E. Quantification of the body weight of the tumor bearing mice that monitored every other day (n=5).